The Effect of Sr Modifier Additions on Double Oxide Film Defects in 2L99 Alloy Castings

QI CHEN and W.D. GRIFFITHS

In this paper, Sr modifier (300 ppm) was added to 2L99 alloy sand castings to investigate its effect on bifilm defects in the castings. Two different sand molds were used in this study, with good and bad running system designs, to introduce different amounts of bifilm defects into the castings. The mechanical properties of the modified 2L99 castings were compared to the properties of unmodified castings and showed that with high bifilm defect contents (H) the Sr addition reduced the Weibull modulus of the UTS by 67 pct and the Position Parameter by 5 pct, and introduced a bimodal distribution into the Weibull plot of the pct Elongation. However, for castings with low bifilm defect content (L), the Weibull moduli of both the UTS and pct Elongation were significantly improved (by 78 and 73 pct, respectively) with the addition of Sr. The Position Parameter of the pct Elongation was improved by 135 pct. The results suggested that a desirable modification effect can only be achieved while the bifilm defect content in a casting was low.

I. INTRODUCTION

AL-SI alloys are widely used in the automotive and aerospace industries due to their high strength-to-weight ratio and castability. However, the plate-like coarse Si phase is usually accused of reducing mechanical properties of the alloy. To solve this problem, minor chemical modifications are used to modify the plate-like Si morphology into a fibrous or coral-like morphology so that mechanical properties, especially ductility, are improved.

Various elements are reported to have a modification effect on Si, among which Sr and Na are the most commonly used.[1–3] Ba and Ca[4,5] are also reported to have a similar but reduced effect on Si. Of the commonly used modifiers, Sr remains longer in the melt than Na but is well known for its association with enhanced gas porosity.[6] McDonald et al.[7] investigated porosity in a Sr-treated alloy and found that, at any Si content, porosity was increased when Sr was added. Tiedje et al.[8] suggested that Sr modification would increase the amount of porosity by 5 to 10 times in an Al-Si alloy.

The impurity-induced twinning (IIT) model[9] and twin plane re-entrant edge (TPRE) mechanism[10] are accepted as explaining the modification behavior. Modifier atoms, with a ratio to Si of r (modifier):r (silicon) = 1.646), are selectively absorbed at re-entrant edges, deactivating the preferential Si growth directions. Another explanation would be that the modifier atoms are absorbed at the growth steps of Si crystals, interrupting the current growth of the Si phase. The Si atom was forced to fall into the next available vacancy and its stacking sequence was changed. The formation of twins of the Si phase was also increased. Li et al.[11] observed the absorption of Eu atoms (with r (modifier):r (Si) roughly equal to 1.646) at twin plane re-entrant edges using STEM. Timpel et al.[12] used atom probe tomography and TEM with nanometer resolution to investigate the behavior of Sr in Al-Si alloy and suggested that the segregation of Sr is responsible for the formation of multiple twins restricting the Si growth. Sr modification was successfully simulated by Eiken et al.[13] using 3D phase field simulation, based on the above two mechanisms.

The topic of bifilm defects was raised by Campbell in the 1990s and since then has led to more awareness of liquid metal quality in the casting of light alloys.[14]

Liquid aluminum will readily form a very thin layer of oxide on the surface of the melt. During the process of liquid metal transfer, the surface of the liquid metal may experience some turbulence. If the local velocity of the liquid metal exceeds about 0.5 ms^{-1},[14] the liquid metal can fold over onto it trapping a pocket of gas. This "doubled-over" structure can then be entrained into the bulk melt and carried around by the bulk liquid flow.

QI CHEN and W.D. GRIFFITHS are with the School of Metallurgy and Materials, College of Engineering and Physical Sciences, University of Birmingham, Edgbaston, Birmingham B15 2TT, UK. Contact e-mail: Q.Chen9927@gmail.com

Once solidified, it forms a defect leading to both a reduction and a variation in mechanical properties.

In order to quantify the effect of bifilm defects, mechanical test data from castings are usually fitted into a Weibull distribution. This was proposed by Weibull in 1951.[15] Campbell and Green[16] used a two-parameter Weibull distribution to describe the properties of Al-7Si-0.35 Mg alloy and suggested that the use of a Weibull distribution produced a better data fit compared to a normal distribution. Tiryakioğlu et al.[17] further improved the estimation procedure for the Weibull parameters, with the help of Monte-Carlo simulation, so that the distribution can better represent the mechanical properties of the casting.

Nyahumwa[18] proposed a hypothesis that the entrapped atmosphere in a bifilm defect might be consumed gradually, with initially oxygen and then nitrogen being consumed, and when the majority of the entrapped atmosphere was depleted, the unwetted sides of the bifilm defects might close and bond together, reducing the detrimental effect of bifilm defects.

It has been suggested that the addition of modifiers might change the oxidation behavior of liquid Al-Si alloys.[19–21] A Sr-related oxide might be formed in Al-Si alloy as observed by Jacob et al.,[21] which are thick (as thick as 500 nm) and non-uniform in thickness. Emadi et al.[20] suggested that the oxidation rate was accordingly increased by three times when Sr was added into an Al-Si alloy. The changed oxidation behavior of liquid aluminum alloy might then alter the behavior of the oxide skin and hence the consumption of the entrapped atmosphere within a bifilm defect which, in turn, might affect the mechanical properties of the casting.

The behavior of bifilm defects in the casting might be affected in a Sr-modified casting.[22] Reiszadeh et al.[23] suggested that the addition of Sr reduced the rate of consumption of the air trapped in a bubble held in the melt and would have the same effect in a bifilm defect. Nateghian[24] suggested that, with the addition of 0.05 wt pct Sr to commercial purity aluminum, the Al2O3 layer started to transform into SrO. Farhoodi et al.[25] suggested that such a transformation might make a bifilm defect stronger which would produce less rupture points and thus the entrapped atmosphere was less likely to be consumed. In this case, a bifilm defect should last longer in an aluminum melt containing Sr (and contribute to increased porosity in the aluminum castings). However, no evidence supporting such a hypothesis was provided.

Another side effect of the addition of Sr was the formation of Sr-containing intermetallic compounds. These intermetallic compounds might be nucleated on a bifilm defect. Miresmaeili[26] calculated the lattice mismatch between $MgAl_2O_4$ spinel and Al_2Si_2Sr to be 4.26 pct, and suggested that spinel could be a favored nucleation site for the growth of intermetallic compounds.

In this work, two designs of sand mold were used to produce castings with higher and lower amounts of bifilm defects. The interaction between additions of the modifier Sr and bifilm defects was investigated by comparing the change in mechanical properties of castings from the two sand mold designs.

II. EXPERIMENTAL PROCEDURE

Castings with higher bifilm defect contents were achieved by casting the mold design shown in Figure 1. The splashing associated with the liquid metal transfer during mold filling should have introduced many bifilm defects into the liquid metal to produce bifilm-rich castings. Oxide film defects formed earlier, during the metal melting stage or residual from the metal ingot and carried into the casting (termed 'old bifilm defects'), would also contribute to the bifilm defect population in the castings. 8 molds were cast of 2L99 alloy (to give 77 test bars), and 3 molds were cast with 2L99 + 300 ppm Sr, to give 30 test bars containing Sr. The molds were made one week prior to casting to allow the evaporation of hydrogen-containing volatiles from the resin binder.

To produce castings with a reduced amount of bifilm defects, the mold design shown in Figure 2 was used. A 20 ppm filter was placed in the cente of the runner bar at the bottom of the downsprue (labeled in Figure 2), which would have the effect of filtering out some of the previously introduced bifilms, and would also reduce the velocity of the liquid metal entering the mold. In these experiments, 3 molds each were cast in 2L99 alloy, and with 2L99 alloy modified by an addition of 300 ppm Sr, giving 30 test bars each.

The liquid metal was poured at 725 °C (998 K). Before that, Argon gas was bubbled from the bottom of the liquid metal to degas for 20 minutes. For the casting with poor running system design, a cooling stick was subsequently inserted into the downsprue as long as the metal was cast. The molds were then rolled 180 degree. This was to allow the proper feeding of the test bar from the running system. The castings were subject to a T6 heat treatment, consisting of a 540 °C (813 K) solution treatment for 12 hours, followed by quenching in hot water at 65 °C (338 K) and by precipitation hardening for 3.5 hours at 155 °C (428 K).

Table I lists the chemical composition of the alloys used in the casting experiments. The pickup rate of the modifier in the casting was confirmed by measurement of their composition using Inductively Coupled Plasma Mass Spectrometry (ICP-MS). This suggested that the Sr addition had a full recovery rate, giving a Sr content of 0.03 wt pct in the castings with both high and low bifilm defect content.

The composition of the alloy in the case of other elements that might affect the variability of mechanical properties (i.e., Mg and Fe) was determined using a Tiger S8 WDXRF (see Table II), which suggested that the Fe and Mg contents were all controlled within an acceptable range with Fe < 0.12 wt pct and Mg 0.3 ± 0.03 wt pct.

Hydrogen content analysis by LECO™ (shown in Table III) suggested that the castings also had similar hydrogen contents, of about 0.17 ± 0.03 ppm.

A section of the running system from each casting was cut and polished, to 0.25 μm, using standard techniques for optical microscopy and examined using a Leica
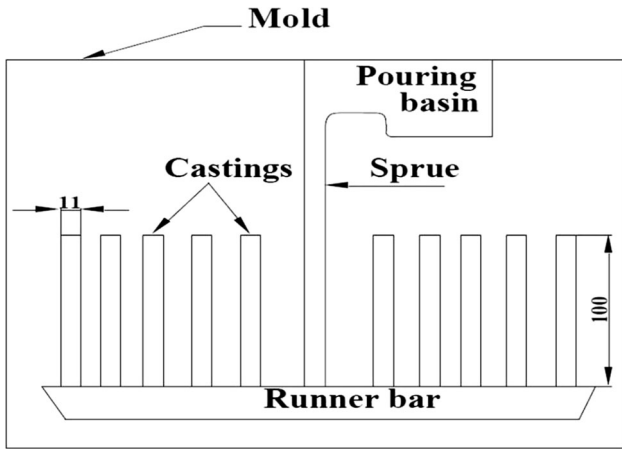

Fig. 1—A diagram showing the running system design of the test bar mold used in the experiments to generate high double oxide film defect content in the test bar castings.

Optical Microscope. Figure 3 shows the morphology of the eutectic Si phase in the castings. Figure 3(a) shows an acicular shaped Si phase in the unmodified 2L99 alloy but was fully modified into a coral morphology with much smaller size, as shown in Figure 3(b).

The cast test bars were machined to produce a gage length of 37 and 6.75 mm in diameter. The radius of the shoulder of the gage length was 26 mm. Tensile testing was conducted using a Zwick tensile testing machine at a strain rate of 1 mm/min, with the UTS and pct Elongation of each test bar recorded. The mechanical properties of the test bars from the unmodified 2L99 castings and modified 2L99 castings were compared for both casting types.

The difference in the amount of bifilm defects was confirmed by examination of the fracture surfaces of 30 test bars (representing 3 molds) from each composition using a Leica X200 camera. The size of the bifilm defect(s) on each fracture surface was measured using ImageJ. The fracture surfaces of the tensile test bars were further observed using a JEOL 7000 Scanning Electron Microscope (SEM), equipped with Oxford INCA EDX.
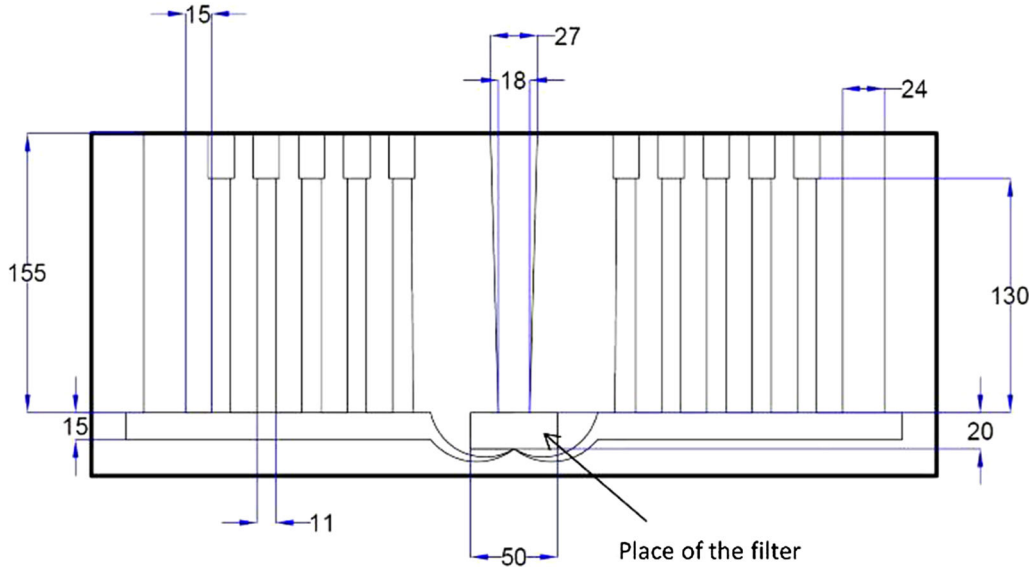

Fig. 2—A diagram showing the running system design of the test bar mold used in the experiments to generate reduced double oxide film defect content in the test bar castings.

Table I. Composition of the 2L99 Alloy Used in the Experiments

Element	Si	Fe	Cu	Mn	Mg	Cr	Ni	Zn	Pb	Sn	Ti	Al
Composition	7	0.1	0.01	0.01	0.34	0.01	0.01	0.01	0.01	0.01	0.1	bal.

Table II. Chemical Composition of the Castings, Measured by XRF

	Castings with High Bifilm Content		Castings with Low Bifilm Content	
Element	2L99 + Sr	2L99	2L99 + Sr	2L99
Fe (wt pct)	0.1	0.1	0.1	0.09
Mg (wt pct)	0.3	0.32	0.32	0.33

The tensile test results for each set of test bars were fitted using a two-parameter Weibull distribution, using linear regression, and the Weibull parameters evaluated to obtain their shape parameter (*i.e.*, the Weibull modulus, showing the scatter of the results) and scale parameter (*i.e.*, the Position Parameter, within which $1 - 1/e$ (63.4 pct) of the data might fail). The cumulative distribution function of the two-parameter Weibull distribution used here is given by Eq. [1]:

$$P = 1 - e^{-\left(\frac{x}{x_0}\right)^m},\qquad [1]$$

where P is the probability of failure, x the measured data point (*e.g.*, UTS, pct Elongation, *etc.*), x_0 the position parameter, and m is the Weibull modulus.

The probability of failure of the samples was unknown and was obtained using the estimation equation as follows[27]:

$$P = \frac{n_i - 0.5}{n + 0.25},\qquad [2]$$

where P is the probability of sample failure, n_i the sample rank, and n is the total sample size.

III. RESULTS

A. *Statistical Analysis of the Weibull Moduli*

Weibull plots for high and low bifilm defect-containing castings are shown in Figure 4. In this work, R^2 was used to assess the goodness of fit of the Weibull distribution for a data set. The tensile test results from the casting can only be accepted as following a Weibull distribution if $R^2 > R^2_{0.05}$. $R^2_{0.05}$ has been shown in

Table III. Hydrogen Analysis Results, Measured by LECO^{TM}

	High Bifilm Content (ppm)	Low Bifilm Content (ppm)
2L99 + Sr	0.182	0.138
2L99	0.197	0.192

Eq. [3], suggested by Tiryakioğlu *et al.*,[28] with sample size n: 1 to 100 and 95 pct confidence. $R^2_{0.05}$ and R^2 values for various castings are shown in Table IV. A summary of the tensile test results is provided in Tables V and VI.

$$R^2_{0.05} = 1.0637 - \frac{0.4174}{n^{0.3}}\qquad [3]$$

If the data set was accepted as having a Weibull distribution, a statistical method was used to compare the difference of Weibull moduli (shape parameter) between modified castings and unmodified castings with
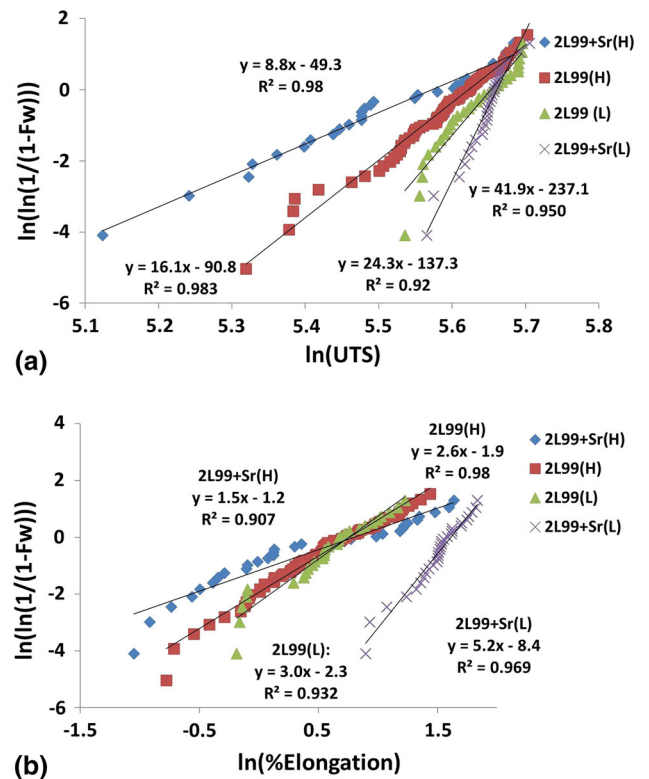

Fig. 4—Graphs of the Weibull plots for (a) UTS and (b) pct Elongation for 2L99 castings, with and without Sr modification, in castings containing both high (H) and Low (L) bifilm defect content.
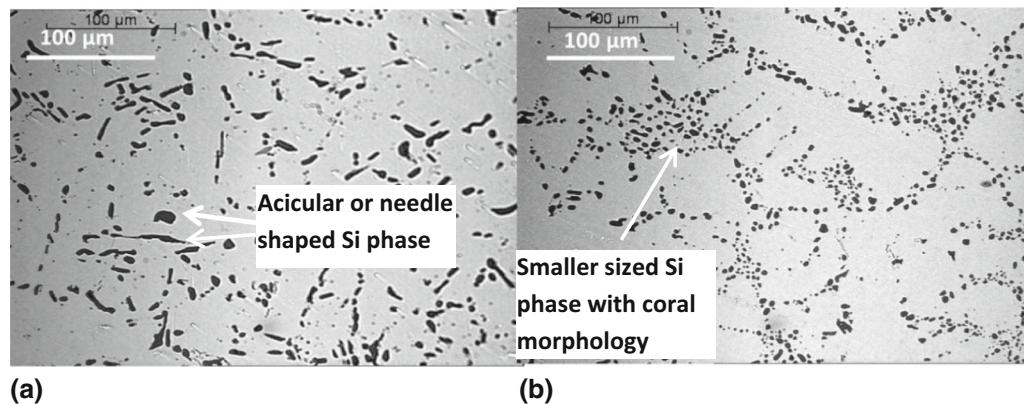

Fig. 3—Morphology of the Si phase in (a) 2L99 alloy and (b) 2L99 castings modified with Sr.

Table IV. A Table of R^2 Values Showing the Goodness of Fit for the Data from the Different Castings

	Casting with High Bifilm Content		Casting with Low Bifilm Content	
	2L99 + Sr	2L99	2L99 + Sr	2L99
Sample size	30	77	30	30
$R^2_{0.05}$	0.91	0.95	0.91	0.91
R^2 value for UTS	0.9811	0.9837	0.9494	0.9305
Accepted as Weibull distribution	yes	yes	yes	yes
R^2 Value for pct Elongation	90.65 pct	96.14 pct	95.66 pct	93.24 pct
Accepted as Weibull distribution	no	yes	yes	yes

Table V. Summary of the Ultimate Tensile Strength Values from the Tensile Test Results

	High Bifilm Defect Content (H)		Low Bifilm Defect Content (L)	
	2L99 + Sr	2L99	2L99 + Sr	2L99
Mean (MPa)	248.41	270	283.6	278.07
Position parameter (MPa)	262.99	277	287.5	284.88
Standard deviation	32.29	15.3	8.1	14.3
Weibull moduli	8.86	16.15	41.9	23

Table VI. Summary of the Percent Elongation Values from the Tensile Test Results

	High Bifilm Defect Content (H)		Low Bifilm Defect Content (L)	
	2L99 + Sr	2L99	2L99 + Sr	2L99
Mean (pct Elongation)	2	1.9	4.59	1.88
Position parameter (pct Elongation)	N/A	2.13	5	2.13
Standard deviation	1.47	0.86	0.97	0.7
Weibull moduli	N/A	3.01	5.24	3.02

Table VII. Statistical Analysis of the Weibull Moduli of the 2L99 Alloy and Sr-Modified 2L99 Alloy Castings

	High Bifilm Defect Content (H) 2L99, 2L99 + Sr	Low Bifilm Defect Content (L) 2L99, 2L99 + Sr
Sample size (n_1, n_2; $n_1 > n_2$)	77, 30	30, 30
2.5 and 97.5 percentiles	0.67, 1.502	0.596, 1.677
m_1/m_2 value (UTS)	1.82	0.58
Statistical difference	yes	yes
m_1/m_2 value (pct Elongation)	N/A	0.58
Statistical difference	N/A	yes

the help of a simulation.[29] Two data sets, with sample size n_1 and n_2 (where $n_1 > n_2$), respectively, were generated with a Monte-Carlo method which followed a Weibull distribution with shape parameter $m = 1$ and scale parameter $\sigma_0 = 3$. The Weibull moduli of the two data sets were evaluated using a linear regression method which gave Weibull moduli of m_1 and m_2. The value of m_1/m_2 was recorded and this process was repeated 100,000 times until a clear distribution was obtained. From this distribution, 2.5 and 97.5 percentiles were obtained.

The ratio of the Weibull moduli of the UTS and the pct Elongation of the 2L99 alloy castings, with and without Sr modifier additions, was determined and, if this value fell between the 2.5 and 97.5 percentiles, then the Weibull moduli of the two castings was assumed to be similar, but if the ratio fell outside the 2.5 and 97.5 percentiles, a statistically significant difference between the two Weibull moduli existed. The corresponding 2.5 and 97.5 percentiles for the different sample sizes used in this work are shown in Table VII.

For the castings with high bifilm defects, this statistical analysis suggested that (see Figure 4, summarized in Tables IV through VII) the Weibull moduli of the UTS showed a statistically significant decrease, from 16.2 to 8.9, when Sr was added into the casting. The R^2 value for the Weibull plot of the pct Elongation was too low for it to be accepted as a Weibull plot. Instead, the Weibull plot showed the presence of two distributions of data, which could be caused by different types of defects accounting for the failure of the samples, perhaps porosity as well as bifilm defects.
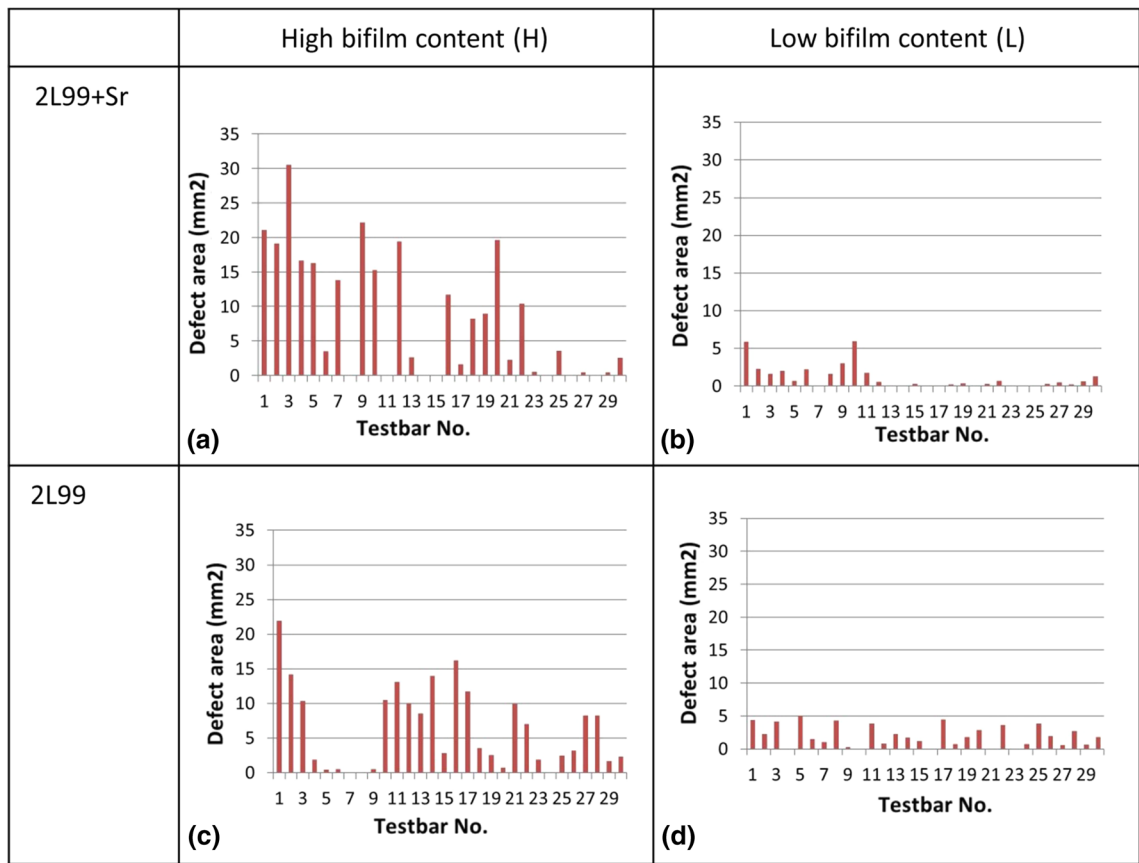
Fig. 5—Histograms showing the measured areas of bifilm defect on the fracture surfaces of (*a*) Sr-modified 2L99 castings with bifilm defect content (H), (*b*) Sr-modified 2L99 castings with low oxide film defect content (L), (*c*) 2L99 casting with high oxide film defect content (H), and (*d*) 2L99 casting with low oxide film defect content (L).
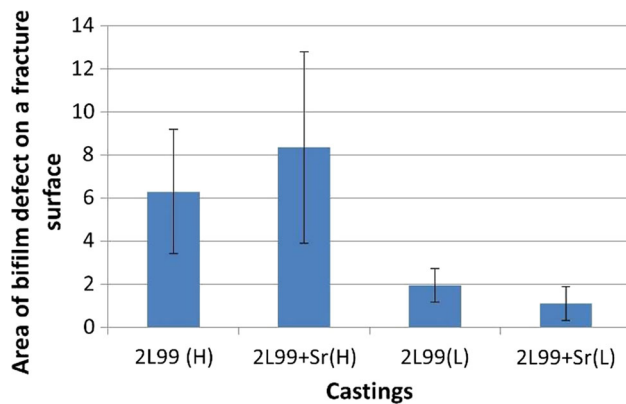

Fig. 6—Histograms showing the mean value of the bifilm defect measured on the fracture surface of the castings shown in Fig. 5.

When the bifilm content in the casting was lower (*i.e.*, the castings with the better mold design shown in Figure 2), the addition of Sr tended to have a strong positive effect on mechanical properties. The Weibull plots are shown in Figure 4, and the results are summarized in Tables IV through VII, showing that the addition of Sr shifted the Weibull moduli of the UTS from 24 to 42. The corresponding value for the pct Elongation was increased from 3.0 to 5.2. Analysis

suggested that both improvements were statistically significant.

B. *Quantification of Bifilm Defect Size on the Fracture Surfaces*

A histogram of the areas of the bifilm defects in the castings is shown in Figure 5. For castings with high bifilm defect content (no modification, Figure 5(c)), the mean bifilm defect size on the fracture surface was about 6 pct of the total cross-sectional area of the samples. This number decreased to about 2 pct in the castings with low bifilm defect content (no modification, Figure 5(d)). A similar trend was seen in the Sr-modified castings. The mean bifilm defect size on the fracture surface decreased from about 8 pct to about 1 pct when the bifilm defect content in the casting was reduced. This confirmed that the use of two different mold designs had resulted in different bifilm defect contents in the castings. The comparisons of the mean value of the size of the bifilm defects on the fracture surfaces in the various castings are shown in Figure 6.

C. *Fracture Surface Analysis of the Cast Test bars*

Figures 7 and 8 show examples of fracture surfaces of 2L99 and 2L99 + Sr alloy test bars, with both high and low bifilm defect contents, respectively. For the castings
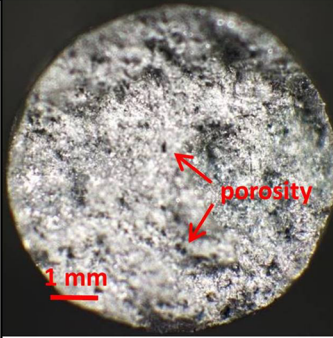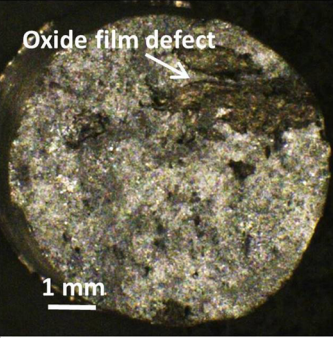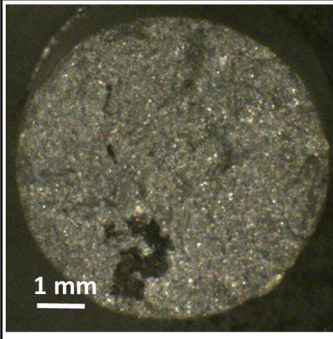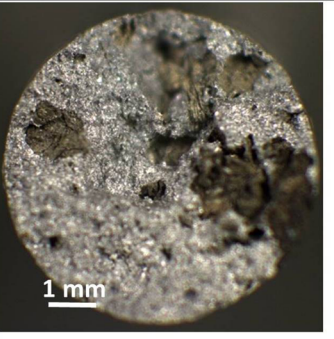
Castings	With good mechanical properties	With average mechanical properties	With bad mechanical properties
2L99+Sr(H)			
Main defect in the casting	porosity (294 MPa, 4.94% Elongation)	oxide film defect (243 MPa, 1.35 %Elongation)	oxide film defect(189 MPa 0.4% Elongation)
2L99(H)			
Main defect in the casting	oxide film defect (284 MPa, 2.86%)	oxide film defect (269 MPa, 1.78% Elongation)	oxide film defect (218 MPa, 0.50% Elongation)

Fig. 7—Optical microscopy images showing examples of the fracture surfaces of unmodified and Sr-modified 2L99 alloy castings, with high numbers of bifilm defects.

with high bifilm content (Figure 7), a bifilm defect was the main reason for failure in all three representative images (good, average, and poor mechanical properties) for 2L99 alloy (2L99(H)). With Sr addition (2L99 + Sr(H)), however, large sized bifilms occurred only on fracture surfaces with poor and average mechanical properties. For the test bar with good mechanical properties, porosity contributed to the failure of the test bars.

For the castings with low bifilm defect content, smaller bifilm defects were observed, with porosity on almost all of the fracture surfaces of the 2L99 + Sr tensile test bars.

SEM and EDX analyses showed two types of defects on test bar fracture surfaces from modified castings, oxide film defects and porosity (shown in Figure 9). This might also explain the tendency for the bimodal distribution of the mechanical properties of 2L99 + Sr castings (shown in Figure 4, having high bifilm defect content). A Sr peak was not detected on the bifilm defect by EDX, which suggested that Sr might not have altered the oxides, or had a very weak effect on the oxide formation process

Figure 10 shows a polished surface from a 2L99 alloy casting, modified with Sr, containing a high quantity of bifilm defects. EDX analysis at site X1 showed an oxygen peak, which suggested the presence of a double oxide film defect. Bright-contrast particles were seen on the sides of the bifilm defects, and EDX analysis (site X2) suggested that they might be Sr-containing intermetallic compounds. Table VIII shows a few composition analyses of the Sr-containing intermetallic compound, which suggested the composition of Al_2Si_2Sr.

IV. DISCUSSION

The lowest Weibull Modulus for the UTS ($m = 9$) was associated with the high-bifilm content castings, to which had been added 300 ppm of Sr (see Figure 4). A slightly higher Weibull modulus of $m = 16$ was obtained when no Sr was added, with the same casting design. This suggests that in castings with poorly designed running systems, and hence high bifilm contents, a Sr modification treatment might be detrimental and lead to an increase in the scatter in mechanical properties. A slight reduction in mechanical properties of about 5 pct, with a Sr addition (judged by the Position Parameter), was also suggested (see Table V).
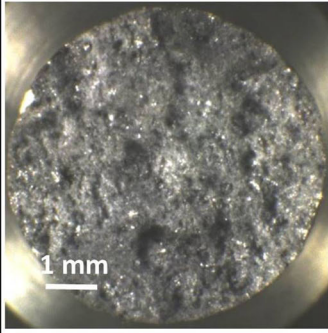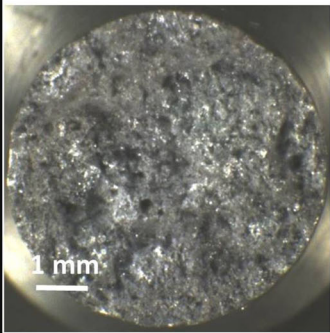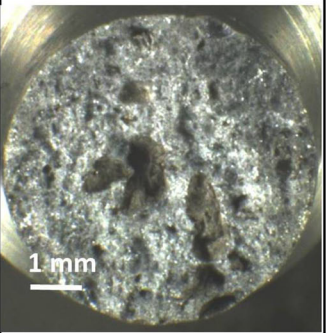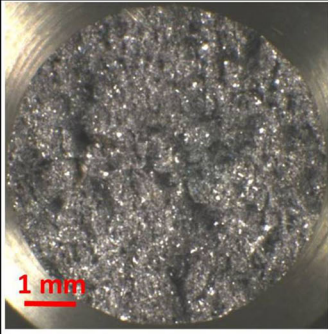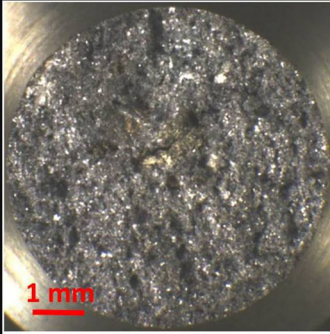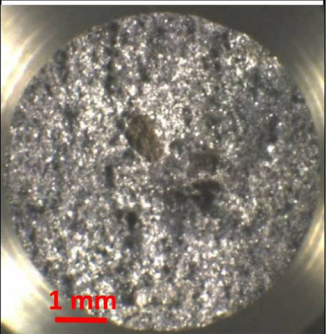
Castings	With good mechanical properties	With average mechanical properties	With bad mechanical properties
2L99+Sr(L)			
Main defect in the casting	(291 MPa,6.0% Elongation)	Porosity(273 MPa, 4.0% Elongation)	Bifilm defect/porosity(261 MPa, 2.45% Elongation)
2L99(L)			
Main defect in the casting	(289 MPa, 2.6% Elongation)	Bi-film defect(275 MPa, 1.93%Elongation)	Bi-film defect (254 MPa, 0.91%Elognation)

Fig. 8—Optical microscopy images showing examples of the fracture surfaces of unmodified and Sr-modified 2L99 alloy castings, with low numbers of bifilm defects.

Table VIII.   Composition of the Sr-Containing Intermetallic Compound, Measured by EDX

	At. Pct			
	No.1	No.2	No.3	No.4
Al	42	41	45	45
Si	39	40	37	37
Sr	19	19	18	18

The decrease in Weibull modulus of the UTS can be attributed to the addition of Sr, although several mechanisms by which this effect occurs are possible, with several mechanisms occurring simultaneously also possible. (i) The addition of Sr may have resulted in an increase in the bifilm content, since the Sr addition was made using an Al-Sr master alloy stirred into the melt, which may have therefore introduced more double oxide film defects into the liquid alloy. Although the similarity in area of defects on the fracture surfaces suggests that this might not be a great effect (see Figure 5), there does appear to be more variability in the defect areas on the fracture surfaces of castings with Sr modification (compare Figures 5(a) and 5(c)). The highest bifilm defect content observed on a single test bar (associated with the lowest UTS) constituted about 80 pct of the fracture surface for the Sr addition casting, compared with about 60 pct for the Sr-free castings. In addition, 9 test bars were seen to contain a bifilm defect content higher than 40 pct of the fracture surface in the Sr-containing casting, compared with only 2 test bars in the Sr-free castings. The larger oxide film defects in the Sr-modified casting might be associated with poorer mechanical properties which contributed to a low Weibull modulus (as the Weibull modulus was quite tail sensitive). (ii) The addition of Sr should have altered the eutectic Si morphology (see Figure 3). An improvement in fineness of the eutectic Si particles would
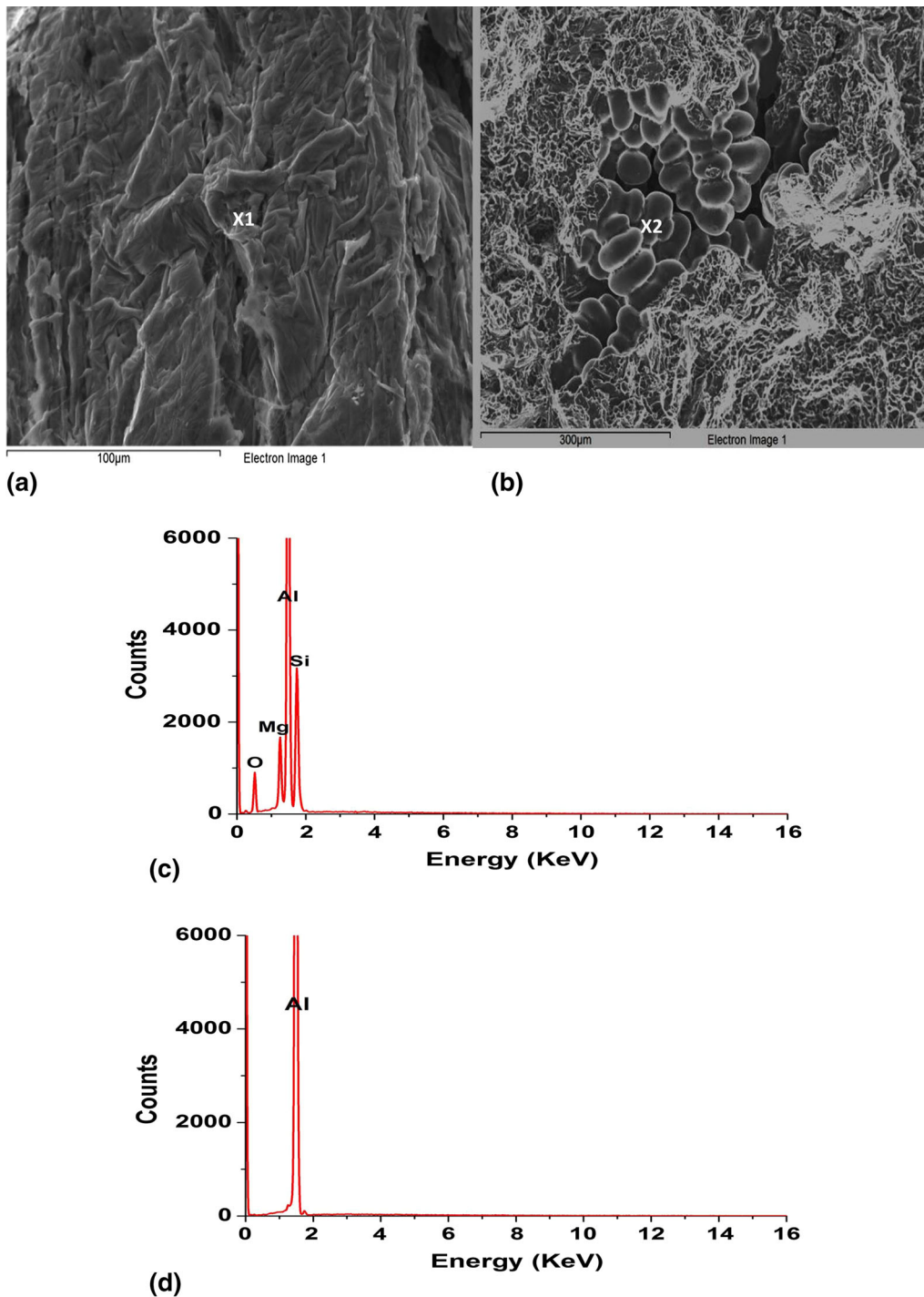
Fig. 9—SEM micrographs showing (a) an oxide film defect and (b) porosity, found on the fracture surfaces of 2L99 castings modified with Sr; (c) and (d) The associated EDX spectra obtained from the points labeled X1 and X2 (Sr peak should occur at 14.1 KeV).

improve the mechanical properties and reduce the variation in mechanical properties (but by an amount difficult to deduce). However, no increase in UTS was noted in comparing these results, although pct Elongation was increased by about 3 pct with the Sr addition (see Table VII). This could be because the detrimental effect of high bifilm defects introduced into the casting played a more important role in determining the

mechanical properties compared with the beneficial effect from the effect of modification. (iii) Earlier work has suggested a redistribution of solidification shrinkage from macroshrinkage to microshrinkage,[30] which might alter the shrinkage formation position and result in the formation of some of the shrinkage porosities in the test bar (which the original mold designed were to avoid). This may be a contributing factor to the decrease
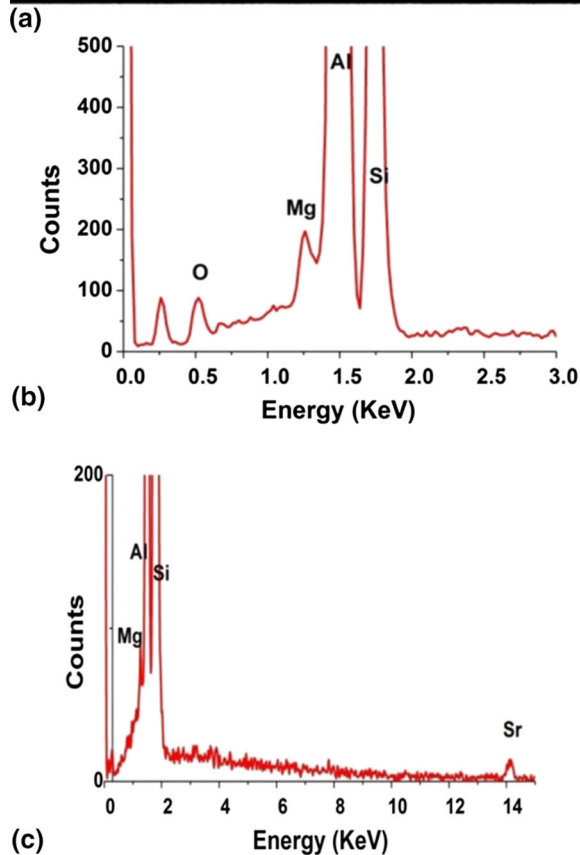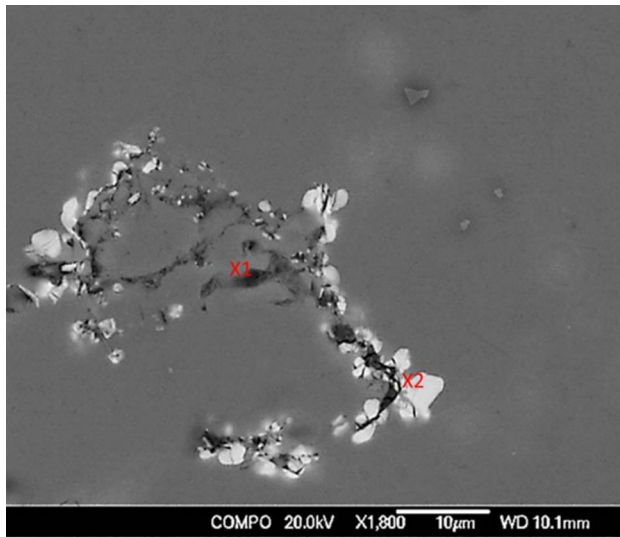
Fig. 10—(a) An example of a SEM micrograph of a polished cross-section surface of a Sr-modified 2L99 alloy, from a high-bifilm content casting, showing Sr-containing intermetallic compound growing on the sides of a double oxide film defect; (b) and (c) with the associated EDX spectrum at the points labeled X1 and X2 respectively.

in Weibull Modulus associated with Sr. (iv) Figure 10 shows intermetallic compounds (possibly Al_2Si_2Sr) presumed to have been nucleated on a bifilm defect, where many particles are seen growing away from the defect. The presence of the Sr-containing intermetallic particles may have enhanced the detrimental effect of Sr on the alloy, perhaps by acting as a conduit for H to diffuse into the interior atmosphere of bifilms, allowing them to expand, or by virtue of their nucleation relationship with the bifilm, making it act as a more severe defect.

No statistically significant difference was noted in the pct Elongation results (see Table VII), although in the case of the high-bifilm content castings with Sr the results showed tendency for a bimodal distribution (reflecting two different causes of failure, bifilm defects and porosity).

However, the use of a well-designed running system produced an opposite effect. The highest Weibull Modulus for the UTS ($m = 42$) was associated with low-bifilm content castings to which had been added 300 ppm Sr (see Figure 4). A significantly lower Weibull modulus of $m = 24$ was obtained with the same casting design (and hence presumably similar bifilm content) with no Sr addition. (This was also shown in the similarity in the measured area of the bifilms, determined from the fracture surfaces, of 1 and 2 pct, respectively (see Figure 6).)

Figures 7 and 8 show examples of fracture surfaces from the different casting experiments. Oxide film defects were found on fracture surfaces with a low bifilm content, when $m = 24$, but porosity was more frequently observed with low bifilm content castings with Sr added. The high Weibull modulus of 42 is probably attributed to the low bifilm defect content and the transition to a more reproducible size of defect causing failure, namely porosity, which would be more spherical, compared to a two-dimensional type of defect such as a bifilm. The beneficial effect on the mechanical properties by the Si phase modification outweighed the detrimental effect from the casting defects (i.e., bifilm defect and porosity).

No evidence was found for the addition of Sr causing a change in the composition or structure of the bifilm defects. Previous explanations of the role of bifilm defects in affecting mechanical properties have focussed on the reaction of the interior gases with the surrounding melt, reducing their size and reducing their impact on properties.[18,23,31] In these experiments, it has been shown that the use of a good running system design, coupled with a transition to spherical porosity, has resulted in the most reproducible mechanical properties.

V. CONCLUSIONS

1. Tensile test results suggested that the addition of 300 ppm Sr in a high bifilm defect-containing 2L99 alloy tended to have a negative effect on mechanical properties of the castings, reducing the Weibull modulus of the UTS and increasing its variability.
2. When the running system design was changed and the bifilm defect content in the casting was reduced, a significant improvement in the Weibull modulus of the UTS and pct Elongation was seen. The mean value of pct Elongation was also improved by 300 pct.

3. The increased bifilm defect content, increased amount of porosity, and the effect of intermetallic compounds nucleating on the sides of the bifilm defect could all be reasons why an addition of Sr reduced the Weibull moduli of the UTS in a high bifilm-containing 2L99 casting.

4. For castings with a low bifilm defect content, the beneficial effect of the Sr addition was probably due to the effect of Si modification (which outweighed the detrimental effect of double oxide film defects, due to the reduced defect content in the casting).

REFERENCES

1. D. Emadi, J.E. Gruzleski, and J.M. Toguri: *Metall. Trans. B*, 1993, vol. 24 (6), pp. 1055–63.
2. J.E. Gruzleski and B.M. Closset: *AFS Trans.*, 1990, vol. 92, p. 256.
3. S.C. Flood and J.D. Hunt: *Met. Sci.*, 1981, vol. 15 (7), pp. 287–94.
4. A. Knuutinen, K. Nogita, S.D. McDonald, and A.K. Dahle: *Light Met.*, 2001, vol. 1 (4), pp. 229–40.
5. K. Nogita, S.D. McDonald, and A.K. Dahle: *Mater. Trans.*, 2004, vol. 45 (2), pp. 323–26.
6. G. Sigworth: *AFS Trans.*, 1983, vol. 66, pp. 7–16.
7. S.D. McDonald, K. Nogita, and A.K. Dahle: *Acta Mater.*, 2004, vol. 52 (14), pp. 4273–80.
8. N.S. Tiedje, J.A. Tayor, and M.A. Easton: *Metall. Trans. A*, 2012, vol. 43 (12), pp. 4846–58.
9. S.Z. Lu and A. Hellawell: *Metall. Trans. A*, 1987, vol. 18 (10), pp. 1721–33.
10. D.R. Hamilton and R.G. Seidensticker: *J. Appl. Phys.*, 1960, vol. 31, pp. 1165–73.
11. J. Li, F. Hage, M. Wiessner, L. Romaner, D. Scheiber, B. Sartory, Q. Ramasse, and P. Schumacher: *Sci. Rep.*, 2015, vol. 5, p. 13802.
12. M. Timpel, N. Wanderka, R. Schlesiger, T. Yamamoto, N. Lazarev, D. Isheim, G. Schmitz, S. Matsumura, and J. Banhart: *Acta Mater.*, 2012, vol. 60, pp. 3920–28.
13. H. Eiken and M. Apel: *IOP Conf. Ser. Mater. Sci. Eng.*, 2016, vol. 84 (1), p. 12084.
14. J. Campbell: *Complete Casting Handbook*, Butterworth-Heinemann, Oxford, 2011, pp. 19–28.
15. W. Weibull: *J. Appl. Mech. Tran. ASME*, 1951, vol. 18 (3), pp. 293–97.
16. N.R. Green and J. Campbell: *J. Mater. Sci. Eng. A*, 1993, vol. 173 (1), pp. 261–66.
17. M. Tiryakioğlu and D. Hudak: *J. Mater. Sci.*, 2008, vol. 527 (1–2), pp. 397–99.
18. C. Nyahumwa, N.R. Green, and J. Campbell: *AFS Trans.*, 1998, vol. 106, pp. 215–23.
19. H. Iwahori, K. Yonekura, Y. Yamamoto, and M. Nakamura: *J. Jpn. Foundrym. Soc.*, 1989, vol. 61 (10), pp. 730–35.
20. D. Emadi, J. Gruzleski, and M. Pekguleryuz: *AFS Trans.*, 1996, vol. 104, pp. 763–68.
21. S. Jacob: *Fonderie*, 1977, vol. 363, pp. 13–25.
22. J. Campbell and M. Tiryakioglu: *J. Mater. Sci. Technol.*, 2010, vol. 26 (3), pp. 262–68.
23. R. Raiszadeh and W.D. Griffiths: *Metall. Trans. B*, 2006, vol. 37 (6), pp. 865–71.
24. M. Nateghian, R. Raiszadeh, and H. Doostmohammadi: *Metall. Trans. B*, 2012, vol. 43 (6), pp. 1540–49.
25. B. Farhoodi, R. Raiszadeh, and M.H. Ghanaatian: *J. Mater. Sci. Technol.*, 2014, vol. 30 (2), pp. 154–62.
26. S.M. Miresmaeili, J. Campbell, S.G. Shabestari, and S.M.A. Boutorabi: *Metall. Trans. A*, 2005, vol. 36 (9), pp. 2341–49.
27. A. Khalili and K. Kromp: *J. Mater. Sci.*, 1991, vol. 26 (24), pp. 6741–52.
28. M. Tiryakioğlu and J. Campbell: *Metall. Trans. A*, 2010, vol. 41 (12), pp. 3121–29.
29. D. Hudak and M. Tiryakioğlu: *Mater. Sci. Eng. A*, 2011, vol. 528 (27), pp. 8028–30.
30. G.K. Sigworth: *Int. J. Metalcast.*, 2008, vol. 2 (2), pp. 19–40.
31. M.A. El-Sayed, A.G. Salem, A.Y. Kandeil, and W.D. Griffiths: *Metall. Trans. B*, 2014, vol. 45 (4), pp. 1398–1406.